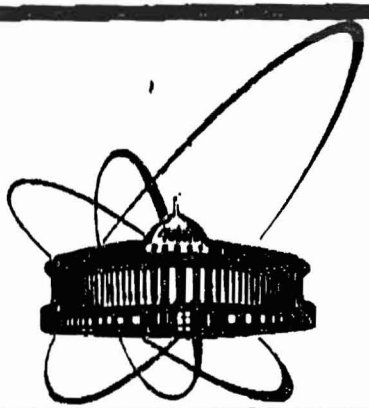

сообщения
объединенного
института
ядерных
исследований
дубна

E17-88-880

W.Salejda*

THE HEAT CAPACITY OF THE ONE-DIMENSIONAL FIBONACCI-TYPE QUASICRYSTALS

*On leave of absence from Institute of Physics, Technical University of Wroclaw, Wybrzeze Wyspianskiego 27, 53-407 Wroclaw, Poland

1988

1. Introduction

Recently, the properties of the electronic and vibrational spectrum of the dynamic models of one dimensional quasicrystals (1D QC) [1,2] are the subject of extensive studies [3,13].

So far, various thermodynamic properties of these systems having the singular continuous spectrum of elementary excitation [4,6,7] have not been investigated in detail.

In this paper we report the numerical results concerning the temperature dependence of the heat capacity C of the one-dimensional Fibonacci-type quasicrystals (1D FQC).

The harmonic models describing the vibrational motions of atoms are used and the next-nearest-neighbour interactions of atoms are taken into account.

The spectrum of the 1D FQC containing $F_{18}=2584 \leqslant N \leqslant F_{21}=10946$ atoms is obtained numerically and used for the calculation of dependencies of the heat capacity C on the reduced temperature T_{RED} in the wide range of T_{RED}.

Moreover, the dependence of the results on the variations of model parameters is studied in detail.

The paper is organized as follows. Specification of the studied models in Sec.2 is given. Sec.3 contains the basic equations. The numerical results and concluding remarks are given in Sec.3.

2. Specification of the models

Let us briefly specify two one-dimensional models considered in this paper.

Model (I). Quasiperiodic binary alloy

The quasilattice (QL) of the one-dimensional Fibonacci-type quasicrystal [1,2] is defined by the set of points $\{x_n\}$ given by

$$x_n = n + \beta + [\, n/\tau + \alpha \,]/\tau . \qquad (1)$$

where α , β are the real numbers, τ is a golden ratio equal to $(1 + \sqrt{5})/2$ and $[y]$ denotes the integer part of y.

We decorate 1D QL placing two types of atoms in the middle of the points given by (1) (with $\alpha=\beta=0$), i.e. the equilibrium position of n-th atom having the mass

$$m_n=m_o(1 + q([(n+1)/\tau]-[n/\tau])) \qquad (2)$$

is

$$l_n = (x_{n+1}+x_n)/2 . \qquad (3)$$

where $q=z/\tau$ is the so-called parameter of quasiperiodicity.

In this chain (see Fig.1) we have: (1) two types of nearest-neighbour (NN) spring constants k_{HL} and k_{HH} ; (2) three types of next-nearest-neighbour (NNN) spring constants g_{HH} , g_{LH} and g_{LL}.

In this paper the 1D harmonic binary chain with quasiperiodic distribution of masses but constant isotropic forces

$$k_{HL}=k_{HH}=k_o \qquad (4a)$$

$$g_{HH}=g_{LH}=g_{LL}=g_o \qquad (4b).$$

is studied.

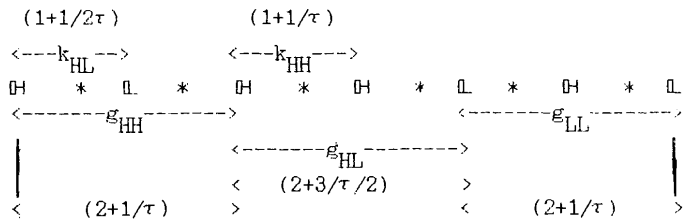

Fig.1. The harmonic interactions of nearest-neighbour (k_{HL} and k_{HH}) and next-nearest-neighbour (g_{HH}, g_{HL} and g_{LL}) atoms in the model (I); the asterisks (*) indicate the points of 1D QL, the letters H and L denote the atoms the masses of which are $m_o(1+q)$ and m_o , respectively; in the parenthesis the dimensionless distances between atoms are given.

Model (II). Pure Fibonacci chain

We decorate QL of 1D QC placing atoms having identical masses ($m_i=m_o$ for all $1 \leq i \leq N$) at the points given by (1) with $\alpha=\beta=0$.

We assume that the strengths of NN and NNN harmonic interactions depend on average lattice distance between atoms. We have chosen $k_{n,n+1}$ and $g_{n,n+2}$ in the following forms (see also Fig.2):

$$k_{n,n+1}=k_o(1+q(1-d_{n,n+1})) \qquad (5)$$

$$g_{n,n+2}=g_o(1+q(2-d_{n,n+2})) . \qquad (6)$$

where

$$d_{n,n+i}=[(n+i)/\tau]-[n/\tau] \ , i=1,2,.... \qquad (7).$$

From (5)-(7) it follows that the large values of $\{k_{n,n+1}\}$ and $\{g_{n,n+2}\}$ correspond to the short distances between NN and NNN atoms in the chain.

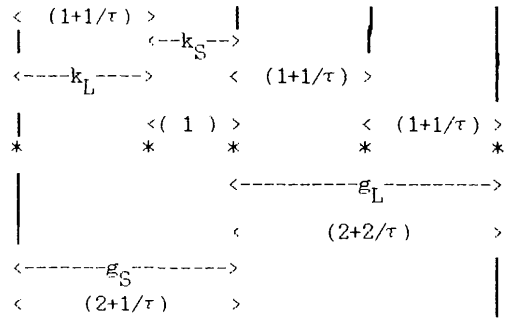

Fig.2. The harmonic interactions of nearest-neighbour ($k_L=k_o$, $k_S=k_o(1+q)$) and next-nearest-neighbour ($g_S=g_o(1+q)$, $g_L=g_o$) atoms in the model (II); in the parenthesis the dimensionless distances between interacting atoms (indicated by asterisks(*)) are given.

Notice, that (2),(5) and (6) define the binary quasiperiodic sequences whose properties have extensively been studied recently by Aviram [14,15].

3. Basic equations

The quantum-mechanical equation of motion of the systems under consideration is

$$\left\{ -\sum_{i=1}^{N} \frac{\hbar^2}{2m_i}\frac{d^2}{du_i^2} + \frac{1}{2}\sum_{i=1}^{N} k_{i,i+1}\,(u_i-u_{i+1})^2 + \frac{1}{2}\sum_{i=1}^{N} g_{i,i+2}\,(u_i-u_{i+2})^2 - E \right\} \Psi = 0 . \qquad (8).$$

The Schroedinger equation (8) can be diagonalized by the normal coordinate transformation (NCT) $\vec{u}=D\vec{Q}$ which also

diagonalizes the classical equations of motion (see below) [16].

Using this NCT the equation (8) can be decomposed into N independent equations for the linear harmonic oscillators

$$\left\{ -\frac{\hbar^2}{2}\frac{d^2}{dQ_i^2} + \frac{1}{2}\omega_i^2 Q_i^2 - E_i \right\} \phi_i(Q_i) = 0 \qquad (9)$$

and the total energy of the chain consisting of N atoms is

$$E = \sum_{i=1}^{N} \hbar\omega_i \left(n_i + 1/2 \right) , \; n_i = 1,2\,3,\ldots \qquad (10).$$

The harmonic frequencies ω_i appearing in (9) and (10) can be obtained from the classical system of equations [16]

$$m_i \frac{d^2u_i}{dt^2} = k_{i,i-1}\left(u_{i-1}-u_i\right) + k_{i,i+1}\left(u_{i+1}-u_i\right) + g_{i,i-2}\left(u_{i-2}-u_i\right) + g_{i,i+2}\left(u_{i+2}-u_i\right) \qquad (11)$$

$$i=1,2,\ldots,N .$$

Introducing mass dependent variables $q_i=\sqrt{m_i}\,u_i$, i=1,2,..N and the notion of normal modes $q_i(t)=q_i^o \exp(i\,\omega\,t)$, the classical system of equations takes the form

$$\Omega^2 q_i = \alpha_i q_i + \beta_{i-1} q_{i-1} + \beta_{i+1} q_{i+1} + \gamma_{i-2} q_{i-2} + \gamma_{i+2} q_{i+2} \qquad (12)$$

$$i=1,2\ldots N ,$$

where the dimensionless eigenfrequencies Ω and the strength of the next-nearest neighbour interactions are given by $\Omega^2 = m_o \omega_o^2 / k_o$ and $h = g_o / k_o$, respectively and

$$\alpha_i = \frac{m_o}{m_i}\left[\frac{k_{i,i-1}}{k_o} + \frac{k_{i,i+1}}{k_o} + \frac{g_o}{k_o}\left[\frac{g_{i,i+2}}{g_o} + \frac{g_{i,i-2}}{g_o}\right]\right] \quad (13)$$

$$\beta_{i+1} = -\frac{k_{i+1,i}\, m_o}{k_o \sqrt{m_i\, m_{i+1}}} \quad (14)$$

$$\gamma_{i+2} = -h\,\frac{g_{i+2,i}\, m_o}{g_o \sqrt{m_i\, m_{i+2}}} . \quad (15)$$

The harmonic frequencies Ω_i are the eigenvalues of the N*N symmetric band matrix $\mathbb{D}$ of width five if the free boundary conditions are applied ($k_{i,j} = g_{i,j} = 0$ if i or j lie outside the range 1 to N inclusive)

$$\mathbb{D}\, q = \Omega^2\, q , \quad (16)$$

where

$$\mathbb{D} = \begin{pmatrix} \alpha_1 & \beta_2 & \gamma_3 & & & & & & \\ \beta_2 & \alpha_2 & \beta_3 & \gamma_4 & & & & & \\ \gamma_3 & \beta_3 & \alpha_3 & \beta_4 & \gamma_5 & & & 0 & \\ & \gamma_4 & \beta_4 & \alpha_4 & \beta_5 & \gamma_6 & & & \\ & & \ddots & & & & & & \\ & & & \ddots & & & & & \\ & & & & & \gamma_{N-2} & \beta_{N-2} & \alpha_{N-2} & \beta_{N-1} & \gamma_N \\ & & 0 & & & & \alpha_{N-1} & \beta_{N-1} & \alpha_{N-1} & \beta_N \\ & & & & & & & \gamma_N & \beta_N & \alpha_N \end{pmatrix} \quad (17)$$

We have diagonalized numerically the dynamic matrix $\mathbb{D}$ using EISPACK routines for the number of atoms $F_{18} \leq N \leq F_{21}$, where $F_{18} = 2584$ and $F_{21} = 10946$ are the Fibonacci numbers.

The obtained numerically eigenvalues Ω_i have been used further to calculate the heat capacity

$$\mathbb{C}(T_{RED}) = \frac{C(T_{RED})}{N\ k_B} = \sum_{i=1}^{N} \frac{\nu_i}{N}\left[\frac{\varepsilon_i / T_{RED}}{1 - \nu_i}\right]^2 , \quad (18)$$

where $\varepsilon_i = \Omega_i / \Omega_{max}$, $\nu_i = \exp(-\varepsilon_i / T_{RED})$, $T_{RED} = k_B T / E_{max}$ and $E_{max} = h\,\Omega_{max}$, where Ω_{max} denotes the maximal value of Ω_i.

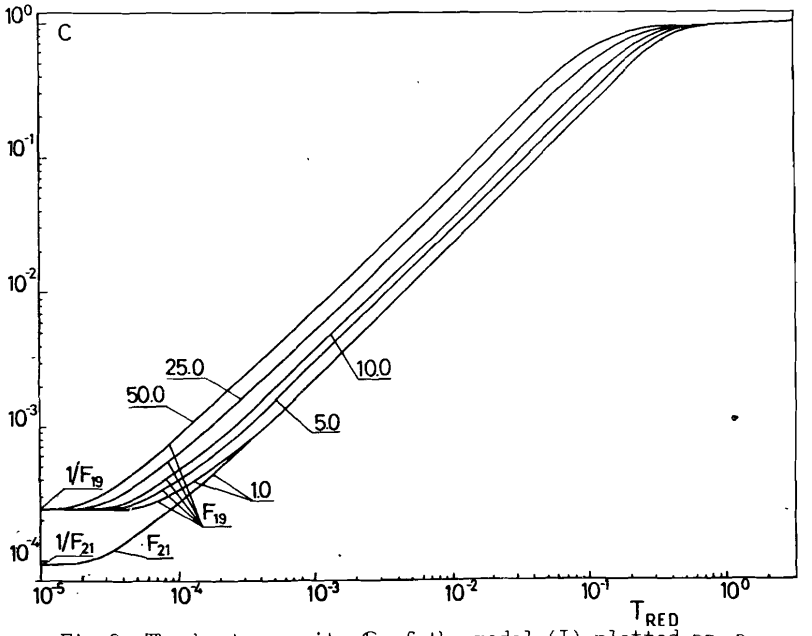

Fig.3. The heat capacity $\mathbb{C}$ of the model (I) plotted as a function of the reduced temperature T_{RED} for the indicated values of z(1.0,5.0,10.0,25.0,50.0); h=0 and the number of atoms N in the chain is F_{19}=4181; for z=1.0 the results obtained for $N=F_{19}$ and F_{21} are presented,too.

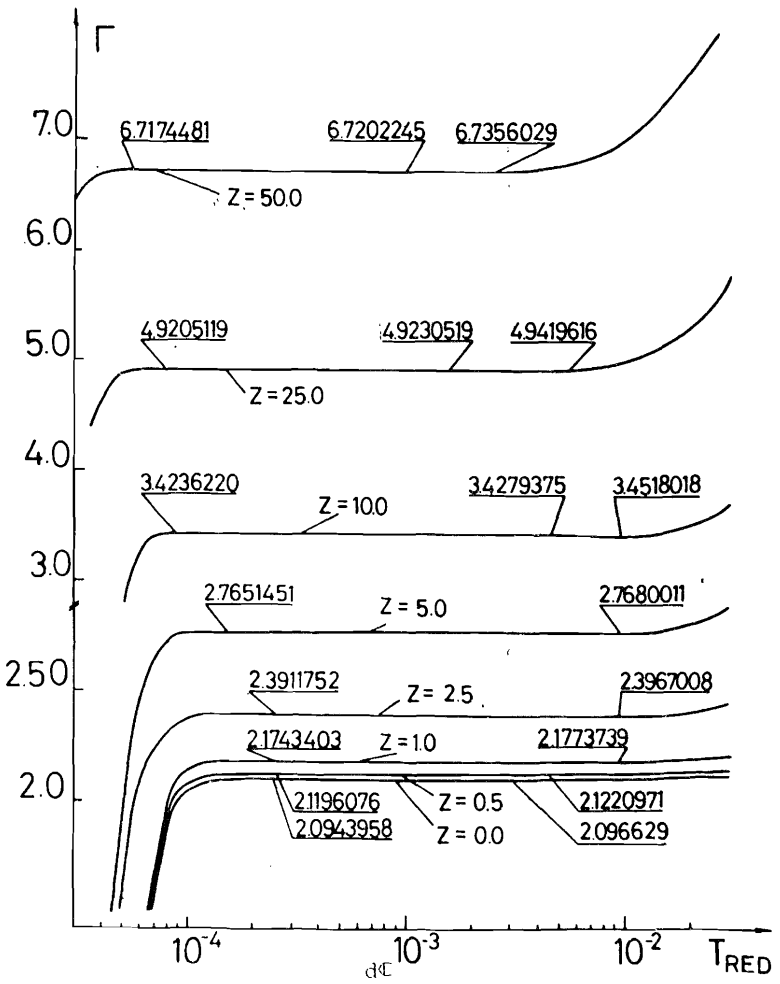

Fig.4.The derivative $\Gamma = \frac{d\mathbb{C}}{dT_{RED}}$ plotted as a function of T_{RED} for the values of z equal to 0.0,0.5,1.0,2.5,5.0,10.0,25.0,50.0; $N=F_{19}$, h=0.0 .

4. Numerical results and discussion

The temperature dependencies of the heat capacity $\mathbb{C}$ and the difference of $\mathbb{C}$ with respect to T_{RED} in Figs.3-6 for the model I and in Figs.7-9 for the model II are presented, respectively.

From the results of our computer simulations the following facts and trends concerning both the models are immediately apparent.

1. At sufficiently low temperatures the heat capacity $\mathbb{C}$ is a linear function of the reduced temperature. There exists the magnitude of T_{RED} below which

$$\mathbb{C}(T_{RED}) = \Gamma(z,h)\, T_{RED} , \qquad (19)$$

where Γ is a constant depending on the model parameters z and h (cf.Figs.3-9).

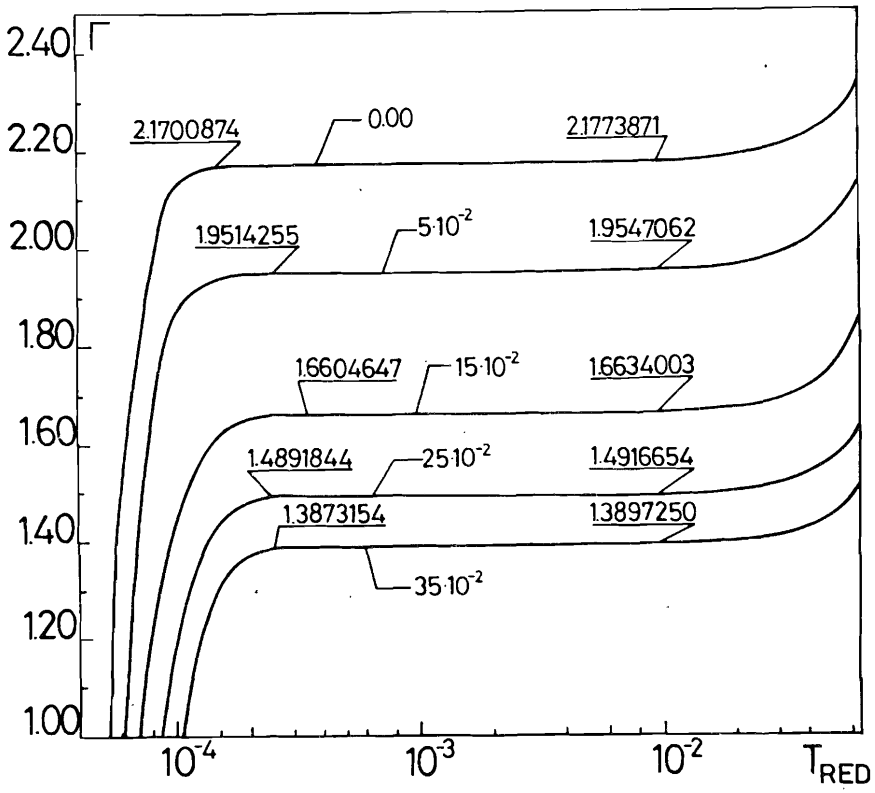

Fig.5. The same as in Fig.4 for $N=F_{19}$, z=1.0 and $0 \leq h \leq 0.35$.

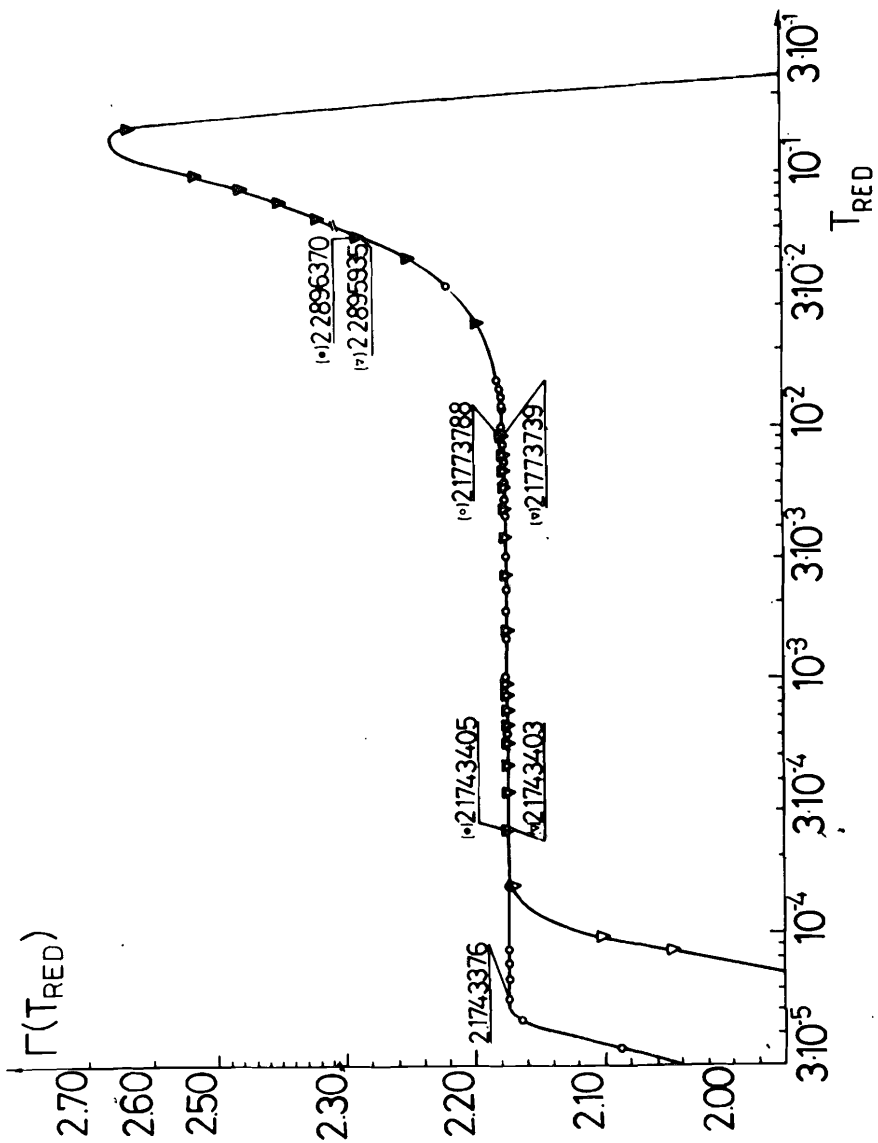

Fig.6. The same as in Fig.4 for $N=F_{19}$ (▽) and $N=F_{21}$ (○), h=0, z=1.0.

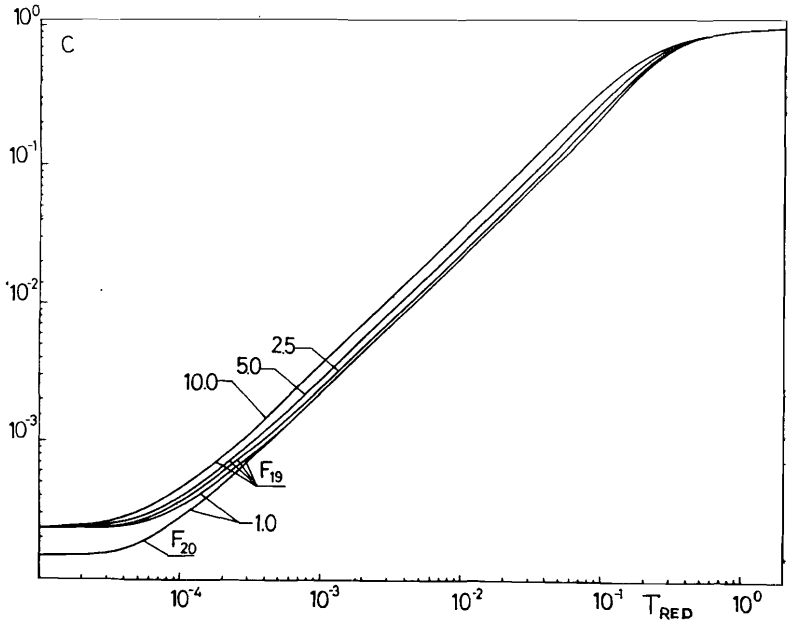

Fig.7. The heat capacity C of the model (II) plotted as a function of the reduced temperature T_{RED} for the indicated values of the parameter of quasiperiodicity z=1.0,2.5,5.0 and 10.0; h=0 and the number of atoms is F_{19}; at z=1.0 the results obtained for $N=F_{19}$ and $N=F_{20}$ are given , too.

In Figs.4-6 and in Figs.8-9 the calculated values of Γ are presented for the models I and II, respectively. The plots show that Γ is almost independent of temperature at $T_{RED} \lesssim 10^{-2}$. Moreover, in Figs.4-6 and 8-9 the beginning (Γ_B) and the end (Γ_E) of each plateau is indicated by the calculated values of Γ. Notice that in the region of plateau the parameter

$$\vartheta = 2 (\Gamma_E - \Gamma_B) / (\Gamma_E + \Gamma_B) \qquad (20)$$

describing the relative slopes of Γ is less than 0.3 %.

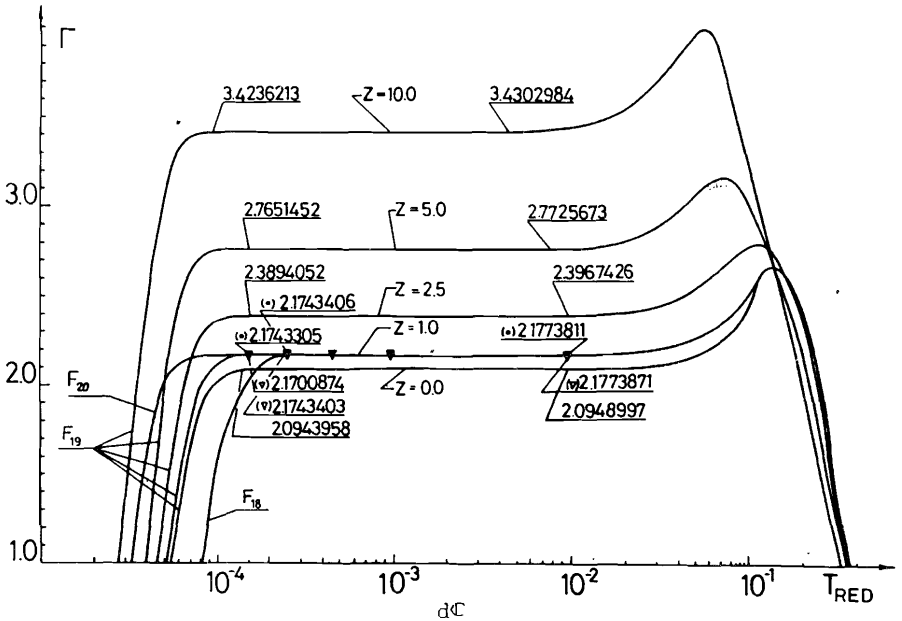

Fig.8. The difference $\Gamma = \frac{d\mathbb{C}}{dT_{RED}}$ plotted as a function of T_{RED} for indicated values of z(0.0,1.0,2.5,5.0,10.0); h=0 and the number of atoms $N=F_{19}$; for z=1.0 the results obtained for $N=F_{18}$, $N=F_{19}$ (▼)and F_{20} (•) are presented,too.

2. At high temperatures, i.e. at $T_{RED} \gg 1$ the heat capacity $\mathbb{C}$ approaches the value given by the Dulong-Petit law.

3. The variation of the models parameter z and h leads to the quantitative changes of $\mathbb{C}$ and Γ. The heat capacity increases with z (cf. Figs.3,4,7,8) and Γ diminishes with increasing of h (cf. Figs.5,9). In addition we observe that the temperature region in which $\mathbb{C}$ depends linearly on T_{RED} shifts to a lower region of the reduced temperature if the parameter z is growing up (cf.Figs.4,8).

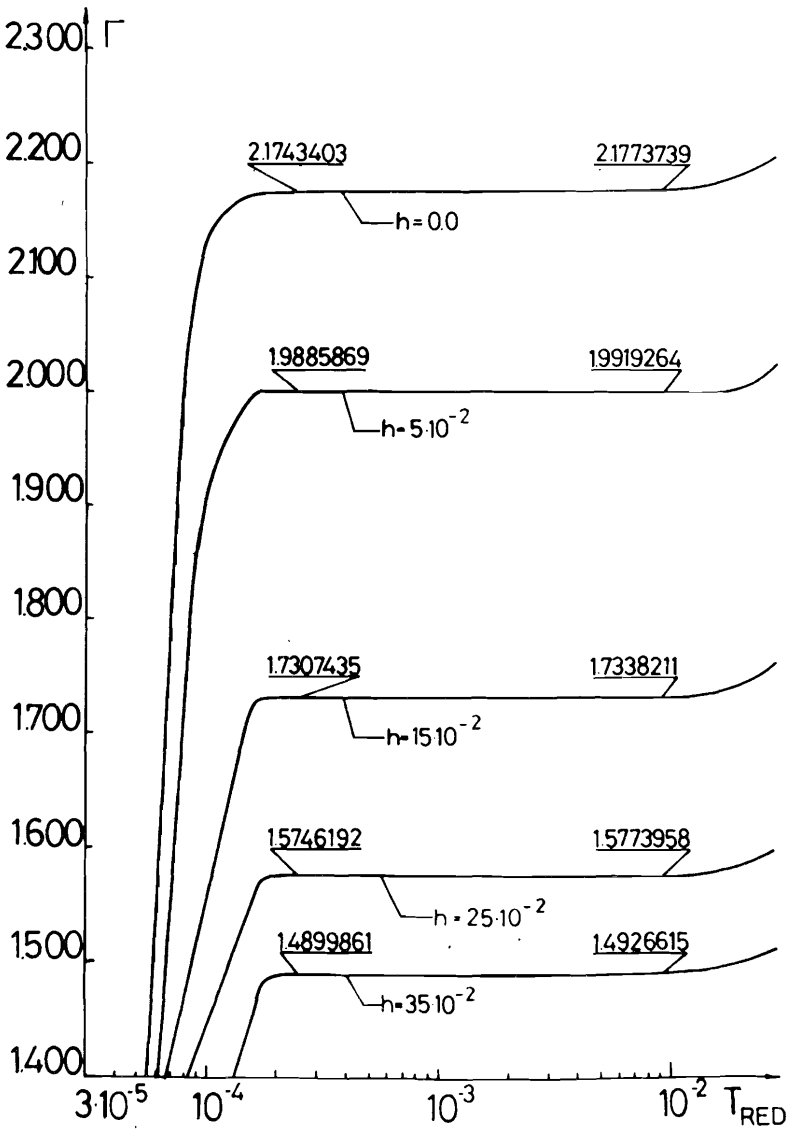

Fig.9. The same as in Fig.8 for $N=F_{19}$ and $0 < h < 0.35$.

We have studied also the finite size effects in $\mathbb{C}$ and Γ. Comparison of the calculated results for various numbers of atoms N in the chain in Figs.3,6 and in Figs.7,8 for the

models I and II are shown, respectively. As has been expected the linear dependence of C on T_{RED} is observed in the wider low-temperature region for the larger values of N. These results confirm our first comment given above.

Finally, let us interpret the obtained numerical results in terms of the integrated density of states $G(\varepsilon_i^2)$.

In the framework of both the studied models we find that [17]:

A1. In the optical region of vibrational spectrum (VS) $G(\varepsilon_i^2)$ exhibits the self-similar structure corresponding to the singular continuous spectrum (Cantor set).

A2. In acoustic region of VS the number of gaps and their sizes tend to zero and $G(\varepsilon_i^2)$ looks like as that of the ideal periodic chain, i.e.

$$G(\varepsilon_i^2) = G(z,h)\ \varepsilon_i^2, \qquad (21)$$

where $G(z,h)$ is a constant depending on the model parameter [17]. Our findings are in agreement with the results of the previous investigations [3-9]. In addition, we find that $G(z,h)$ increases with z and diminishes if the parameter h is growing up [17].

For these reasons we can conclude that the obtained temperature dependencies of the heat capacity of the studied harmonic models of 1D FQC behaves identically as for the periodic chain [18].

Acknowledgments

I would like to thank N.M.Plakida for valuable discussions. I am grateful to T.Paszkiewicz for useful comments. J.Malek helped with some of the numerical work. Computations were done at the Laboratory of Computing Techniques and Automation of the Joint Institute for Nuclear Research.

References

1.D.Levine,P.J.Steinhardt,Phys.Rev.B34,596 (1986)

2.J.E.S.Socolar,P.J.Steinhardt,Phys.Rev.B34,617 (1986)

3.J.P.Lu,T.Odagaki,J.L.Birman,Phys.Rev.B33,4809 (1986)

4.F.Nori,J.P.Rodriguez,Phys.Rev.B34,2207 (1986)

5.J.M.Luck,D.Petritis,J.Stat.Phys.42,289 (1986)

6.M.Kohmoto,J.R.Banavar,Phys.Rev.B34,563 (1986)

7.M.Kohmoto,B.Sutherland,Ch.Tang,Phys.Rev.B35,1020 (1987)

8.Y.Liu,R.Riklund,Phys.Rev.B35,6034 (1987)

9.M.C.Valsakumar,G.Ananthakrishna,J.Phys.C20,9 (1987)

10.S.E.Burkov,J.Stat.Phys.47,409 (1987)

11.H.E.Roman,Phys.Rev.B37,1399 (1988)

12.D.Wurtz,T.Schneider,A.Politi,Phys.Lett.129A,88 (1988)

13.H.De Raedt,T.Schneider,Z.Phys.B71,287 (1988)

14.I.Aviram,J.Phys.A19,3299 (1986)

15.I.Aviram,J.Phys.A20,1025 (1987)

16.P.Dean,Rev.Mod.Phys.44,127 (1972)

17.W.Salejda (in preparation)

18.N.W.Ashcroft,N.D.Mermin, Solid State Physics, Holt,Rinehart and Winston ,New York 1976; Chap.23.

Received by Publishing Department on December 21, 1988.